Progress In Electromagnetics Research Letters, Vol. 13, 173–180, 2010

DIFFRACTION BY A LOSSY DOUBLE-NEGATIVE METAMATERIAL LAYER: A UNIFORM ASYMPTOTIC SOLUTION

G. Gennarelli and G. Riccio

Dipartimento di Ingegneria dell'Informazione ed Ingegneria Elettrica
University of Salerno
via Ponte Don Melillo, Fisciano, Salerno I-84084, Italy

Abstract—A uniform asymptotic solution is presented for evaluating the field diffracted by the edge of a lossy double-negative metamaterial layer illuminated by a plane wave at skew incidence. It is given in terms of the Geometrical Optics response of the structure and the transition function of the Uniform Geometrical Theory of Diffraction, and results easy to handle. Its accuracy is well-assessed by numerical tests and comparisons with a commercial solver based on the Finite Element Method.

1. INTRODUCTION

Double-Negative (DNG) metamaterials (MTMs) are characterized by negative permittivity and permeability simultaneously and can be engineered to have electromagnetic properties not generally found in nature. As a consequence, the number of teams studying DNG MTMs and the number of published papers and books on this topic are both growing exponentially (see [1–3] as example).

Numerical methods can be used to solve scattering problems involving DNG MTMs, but they become very poorly convergent and inefficient when considering structures large in terms of the wavelength. The Geometrical Theory of Diffraction (GTD) represents a very interesting alternative at high frequencies. In this framework, a Uniform Asymptotic Physical Optics (UAPO) solution has been recently derived by the authors for determining the field diffracted by the edge of a lossless DNG MTM planar slab illuminated by a plane wave at skew incidence [4].

Corresponding author: G. Riccio (riccio@diiie.unisa.it).

This paper deals with the extension of the approach presented in [4] to lossy layers. As well-known, the losses are the key problem in both design and applications of modern DNG MTMs [5–7], and therefore they must be taken into account in order to obtain realistic results. To solve the problem here tackled, the DNG MTM planar layer is supposed to be isotropic, homogeneous and modelled as a penetrable half-plane. The proposed UAPO solution for evaluating the diffraction phenomenon is given in terms of the Geometrical Optics (GO) response of the slab and the transition function of the Uniform Geometrical Theory of Diffraction (UTD) [8]. Its accuracy and effectiveness are well-assessed by numerical tests and comparisons with results obtained via COMSOL MULTIPHYSICS® simulations.

2. GEOMETRICAL OPTICS: REFLECTION AND TRANSMISSION COEFFICIENTS

Let us consider a linearly polarized plane wave impinging on a lossy, isotropic and homogeneous DNG MTM slab of infinite extent and thickness d, surrounded by free space (see Fig. 1). The slab is characterized by complex electric permittivity $\varepsilon = -\varepsilon_0(\varepsilon' + j\varepsilon'')$ and magnetic permeability $\mu = -\mu_0(\mu' + j\mu'')$, wherein ε', ε'', μ', μ'' are all positive quantities.

The GO response of the structure is determined by the Fresnel's reflection and transmission coefficients relevant to the parallel ($\parallel$) and perpendicular ($\perp$) polarizations. For the considered case, they can be so expressed:

$$R_{\parallel,\perp} = \frac{\overline{R}_{12_{\parallel,\perp}} + \overline{R}_{23_{\parallel,\perp}} \mathrm{e}^{-j2k_{2z}d}}{1 + \overline{R}_{12_{\parallel,\perp}} \overline{R}_{23_{\parallel,\perp}} \mathrm{e}^{-j2k_{2z}d}} \tag{1}$$

$$T_{\parallel,\perp} = \frac{\overline{T}_{12_{\parallel,\perp}} \overline{T}_{23_{\parallel,\perp}} \mathrm{e}^{-jk_{2z}d}}{1 + \overline{R}_{12_{\parallel,\perp}} \overline{R}_{23_{\parallel,\perp}} \mathrm{e}^{-j2k_{2z}d}} \tag{2}$$

where

$$\overline{R}_{ij_{\parallel}} = \frac{\varepsilon_i k_{jz} - \varepsilon_j k_{iz}}{\varepsilon_i k_{jz} + \varepsilon_j k_{iz}} \tag{3}$$

$$\overline{R}_{ij_{\perp}} = \frac{\mu_j k_{iz} - \mu_i k_{jz}}{\mu_j k_{iz} + \mu_i k_{jz}} \tag{4}$$

$$\overline{T}_{ij_{\parallel}} = \frac{2\varepsilon_i k_{jz}}{\varepsilon_i k_{jz} + \varepsilon_j k_{iz}} \tag{5}$$

$$\overline{T}_{ij_{\perp}} = \frac{2\mu_j k_{iz}}{\mu_j k_{iz} + \mu_i k_{jz}} \tag{6}$$

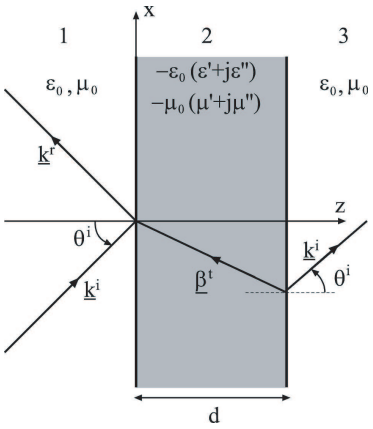

Figure 1. Lossy DNG MTM slab.

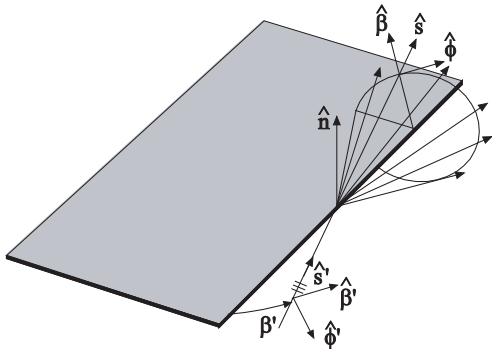

Figure 2. Geometry of the problem.

in which k_{mz} represents the z-component of the propagation vector in the media $m = 1, 2, 3$, and the subscripts i, j refer to the left and right media involved in the local propagation mechanism (see Fig. 1). In particular, $k_{1z} = k_{3z} = k_0 \cos\theta^i$ (k_0 is the free space propagation constant and θ^i is the standard incidence angle), $k_{2z} = -\beta_{2z} - j\alpha_{2z}$ ($\beta_{2z} > 0$ and $\alpha_{2z} > 0$). The phase and attenuation constants in the lossy DNG MTM slab are given by:

$$\beta_{2z} = \sqrt{\frac{B - k_{x1}^2 + \sqrt{A^2 + \left(B - k_{x1}^2\right)^2}}{2}} \tag{7}$$

$$\alpha_{2z} = \sqrt{\frac{-B + k_{x1}^2 + \sqrt{A^2 + \left(B - k_{x1}^2\right)^2}}{2}} \tag{8}$$

with

$$A = k_0^2\left(\varepsilon'\mu'' + \varepsilon''\mu'\right) \tag{9}$$

$$B = k_0^2\left(\varepsilon'\mu' - \varepsilon''\mu''\right) \tag{10}$$

$$k_{x1} = k_0 \sin\theta^i \tag{11}$$

Note that expressions (1) and (2) are in form quite analogous to those reported in [9].

3. UAPO DIFFRACTED FIELD

According to the approach proposed in [4], the analytical difficulties are attenuated by modelling the truncated DNG MTM slab as a half-plane surrounded by free space. The scattering phenomenon produced by an incident plane wave can be analyzed by using the well-known radiation integral with a PO approximation of the involved currents:

$$\underline{E}^s \cong -jk_0 \iint\limits_S \left[\left(\underline{\underline{I}} - \hat{R}\hat{R} \right) \left(\zeta_0 \underline{J}_s^{PO} \right) + \underline{J}_{ms}^{PO} \times \hat{R} \right] G\left(\underline{r}, \underline{r}' \right) \, dS \quad (12)$$

In the above expression, $G(\underline{r}, \underline{r}') = \mathrm{e}^{-jk_0|\underline{r}-\underline{r}'|}/(4\pi|\underline{r}-\underline{r}'|)$ is the Green's function, ζ_0 is the free space impedance, $\underline{r}$ and $\underline{r}'$ denote the observation and source points, respectively, $\hat{R}$ is the unit vector from the radiating element at $\underline{r}\,'$ to the observation point, and $\underline{\underline{I}}$ is the (3×3) identity matrix. The equivalent electric ($\underline{J}_s^{PO}$) and magnetic ($\underline{J}_{ms}^{PO}$) surface currents in (12) can be so determined [4]:

$$\begin{aligned} \zeta_0 \underline{J}_s^{PO} &= \zeta_0 \tilde{\underline{J}}_s^{PO} \mathrm{e}^{jk_0(\rho' \sin\beta' \cos\phi' - \zeta' \cos\beta')} \\ &= \left\{ \left[1 - R_\perp - T_\perp \right] E_\perp^i \cos\theta^i \hat{e}_\perp + \left[1 + R_\parallel - T_\parallel \right] E_\parallel^i \hat{t} \right\} \\ &\quad \mathrm{e}^{jk_0(\rho' \sin\beta' \cos\phi' - \zeta' \cos\beta')} \end{aligned} \quad (13)$$

$$\begin{aligned} \underline{J}_{ms}^{PO} &= \tilde{\underline{J}}_{ms}^{PO} \mathrm{e}^{jk_0(\rho' \sin\beta' \cos\phi' - \zeta' \cos\beta')} \\ &= \left\{ \left[1 - R_\parallel - T_\parallel \right] E_\parallel^i \cos\theta^i \hat{e}_\perp - \left[1 + R_\perp - T_\perp \right] E_\perp^i \hat{t} \right\} \\ &\quad \mathrm{e}^{jk_0(\rho' \sin\beta' \cos\phi' - \zeta' \cos\beta')} \end{aligned} \quad (14)$$

where (ρ', ζ') identify the integration point on the illuminated surface S and $\hat{t} = \hat{n} \times \hat{e}_\perp$, $\hat{e}_\perp$ being the unit vector perpendicular to the standard incidence plane. The angles (β', ϕ') fix the incidence direction, whereas the observation direction is specified by (β, ϕ) in a similar way (see Fig. 2). Since the diffraction is confined to the Keller's cone for which $\beta = \beta'$, the approximation $\hat{R} \simeq \hat{s}$ ($\hat{s}$ is the unit vector of the diffraction direction) for evaluating the edge diffracted field is permitted. As a consequence,

$$\begin{aligned} \underline{E}^s \cong & -jk_0 \left[\left(\underline{\underline{I}} - \hat{s}\hat{s} \right) \left(\zeta_0 \tilde{\underline{J}}_s^{PO} \right) + \tilde{\underline{J}}_{ms}^{PO} \times \hat{s} \right] \\ & \int_0^{+\infty} \int_{-\infty}^{+\infty} \mathrm{e}^{jk_0(\rho' \sin\beta' \cos\phi' - \zeta' \cos\beta')} G(\underline{r}, \underline{r}') \mathrm{d}\zeta' \mathrm{d}\rho' \end{aligned} \quad (15)$$

According to the analytical methodology reported in [4], the UAPO diffracted field results by a uniform asymptotic evaluation and

is given by:

$$\underline{E}^d = \begin{pmatrix} E^d_\beta \\ E^d_\phi \end{pmatrix} = \underline{\underline{D}} \begin{pmatrix} E^i_{\beta'} \\ E^i_{\phi'} \end{pmatrix} \frac{\mathrm{e}^{-jk_0 s}}{\sqrt{s}}$$

$$= \frac{\mathrm{e}^{-j\pi/4}}{2\sqrt{2\pi k_0}\sin^2\beta'} \frac{F_t(2k_0 s \sin^2\beta' \cos^2(\phi \pm \phi')/2)}{\cos\phi + \cos\phi'} \underline{\underline{M}} \begin{pmatrix} E^i_{\beta'} \\ E^i_{\phi'} \end{pmatrix} \frac{\mathrm{e}^{-jk_0 s}}{\sqrt{s}} \quad (16)$$

where s is the distance along the diffracted ray, $F_t(\cdot)$ is the UTD transition function [8], and the sign $+(-)$ applies if $0 < \phi < \pi$ ($\pi < \phi < 2\pi$). The matrix $\underline{\underline{M}}$ is given in [4].

Note that throughout the above discussion an $\mathrm{e}^{j\omega t}$ time dependence has been assumed. On the other hand, if a time factor $\mathrm{e}^{-j\omega t}$ is considered, the corresponding field contributions can be determined by properly conjugating the here reported results.

4. NUMERICAL TESTS

Numerical simulations have been performed to assess the effectiveness of the proposed solution. Figures from 3 to 10 are relevant to a DNG MTM slab having thickness $d = 0.125\,\lambda_0$ and show the field amplitude evaluated over a circular path on the Keller's cone with radius $\rho = 5\lambda_0$, λ_0 being the free space wavelength.

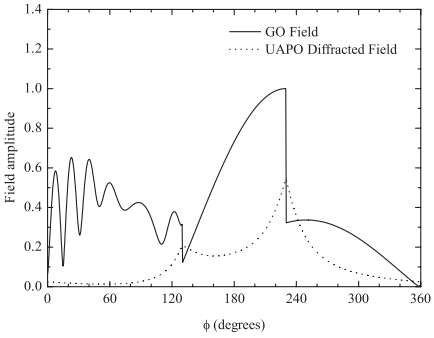

Figure 3. Amplitudes of the electric field β-component of the GO and UAPO contributions. DNG MTM parameters: $\varepsilon' = 4$, $\varepsilon'' = 2$, $\mu' = 1$, $\mu'' = 0.5$. Incident field: $E^i_{\beta'} = 1$, $E^i_{\phi'} = 0$. Incidence direction: $\beta' = 30°$, $\phi' = 50°$.

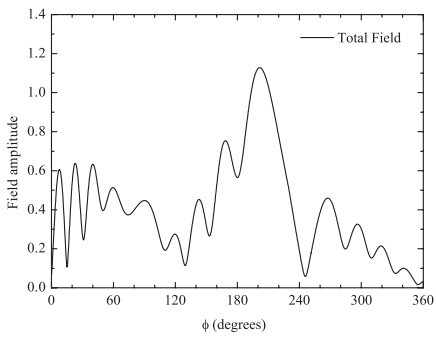

Figure 4. Amplitude of the β-component of the total field. DNG MTM parameters: $\varepsilon' = 4$, $\varepsilon'' = 2$, $\mu' = 1$, $\mu'' = 0.5$. Incident field: $E^i_{\beta'} = 1$, $E^i_{\phi'} = 0$. Incidence direction: $\beta' = 30°$, $\phi' = 50°$.

The GO response and the UAPO diffraction contribution are reported versus ϕ in Fig. 3. Obviously, if $\beta' = 30°$, $\phi' = 50°$, the GO field has two discontinuities in correspondence of the reflection and incidence/transmission shadow boundaries at $\phi = 130°$ and $\phi = 230°$,

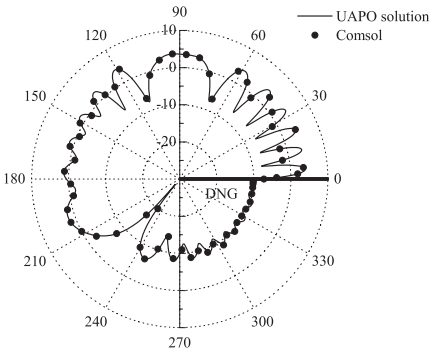

Figure 5. Amplitude (dB) of the β-component of the total electric field. DNG MTM parameters: $\varepsilon' = 4$, $\varepsilon'' = 2$, $\mu' = 1$, $\mu'' = 0.5$. Incident field: $E^i_{\beta'} = 1$, $E^i_{\phi'} = 0$. Incidence direction: $\phi' = 40°$.

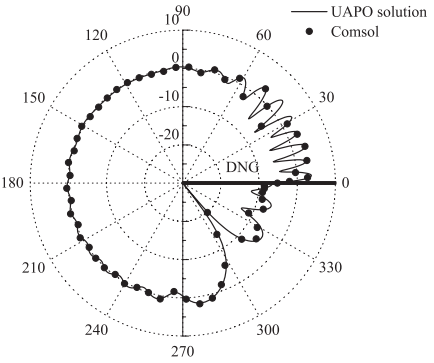

Figure 6. Amplitude (dB) of the β-component of the total electric field. DNG MTM parameters: $\varepsilon' = 4$, $\varepsilon'' = 2$, $\mu' = 1$, $\mu'' = 0.5$. Incident field: $E^i_{\beta'} = 1$, $E^i_{\phi'} = 0$. Incidence direction: $\phi' = 120°$.

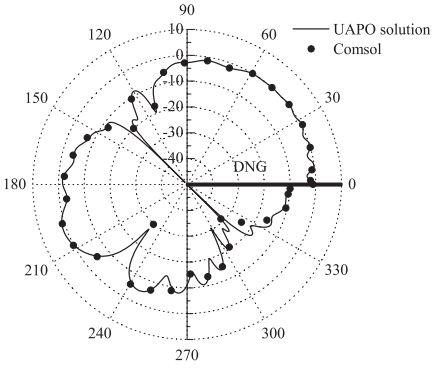

Figure 7. Amplitude (dB) of the ϕ-component of the total electric field. DNG MTM parameters: $\varepsilon' = 4$, $\varepsilon'' = 2$, $\mu' = 1$, $\mu'' = 0.5$. Incident field: $E^i_{\beta'} = 0$, $E^i_{\phi'} = 1$. Incidence direction: $\phi' = 40°$.

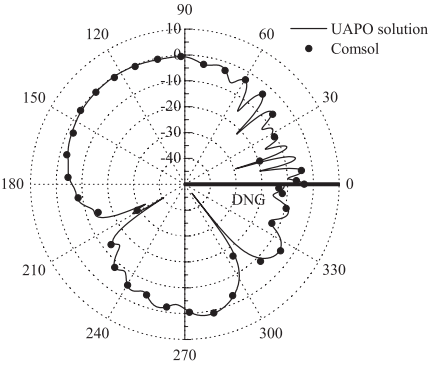

Figure 8. Amplitude (dB) of the ϕ-component of the total electric field. DNG MTM parameters: $\varepsilon' = 4$, $\varepsilon'' = 2$, $\mu' = 1$, $\mu'' = 0.5$. Incident field: $E^i_{\beta'} = 0$, $E^i_{\phi'} = 1$. Incidence direction: $\phi' = 120°$.

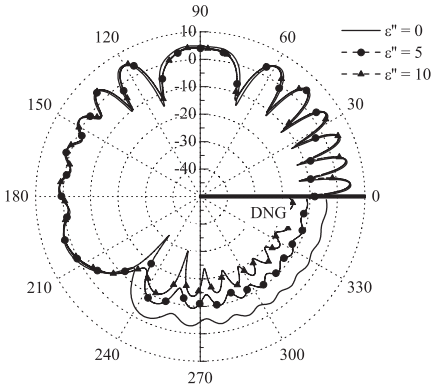

Figure 9. Amplitude (dB) of the β-component of the total electric field. DNG MTM parameters: $\varepsilon' = 4,\ \mu' = 1,\ \mu'' = 0$. Incident field: $E^i_{\beta'} = 1,\ E^i_{\phi'} = 0$. Incidence direction: $\phi' = 40°$.

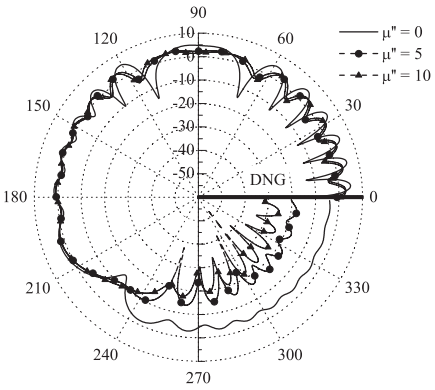

Figure 10. Amplitude (dB) of the β-component of the total electric field. DNG MTM parameters: $\varepsilon' = 4,\ \varepsilon'' = 0,\ \mu' = 1$. Incident field: $E^i_{\beta'} = 1,\ E^i_{\phi'} = 0$. Incidence direction: $\phi' = 40°$.

respectively. The UAPO diffracted field is not negligible in the neighbourhood of such boundaries and ensures the continuity of the total field (see Fig. 4). The proposed UAPO solution has been also tested by means of comparisons with COMSOL MULTIPHYSICS® results in the case of normal incidence (see Figs. from 5 to 8). The excellent agreements confirm its accuracy for both the polarizations.

Finally, the effects of taking electric and magnetic losses into account in the proposed approach are investigated in the next set of figures. In particular, Fig. 9 refers to the presence of electric losses when the incidence angle is less than the right angle. As expected, the field levels in the angular region beyond the incidence/transmission shadow boundary decrease when increasing the relative imaginary coefficient of the complex permittivity. As a matter of fact, this growth produces a reduction of the transmitted field, but it seems to have reduced effects on the reflected field. On the other hand, the growth of the relative imaginary coefficient of the complex permeability appears to influence both transmitted and reflected fields (see Fig. 10).

5. CONCLUSION

The diffraction problem relevant to a lossy DNG MTM slab illuminated by a plane wave at skew incidence has been tackled and solved in

this paper. Numerical examples have demonstrated that the UAPO solution here proposed compensates the GO field discontinuities at the reflection and incidence/transmission shadow boundaries and gives accurate results, as demonstrated by the excellent agreement with COMSOL MULTIPHYSICS® results. The electric and magnetic losses give the impression of affecting the reflected field differently.

REFERENCES

1. Engheta, N. and R. W. Ziolkowski, "A positive future for double-negative metamaterials," *IEEE Trans. Microw. Theory Tech.*, Vol. 53, 1535–1556, 2005.
2. Engheta, N. and R. W. Ziolkowski, *Metamaterials: Physics and Engineering Explorations*, Wiley-Interscience, 2006.
3. Caloz, C. and T. Itoh, *Electromagnetic Metamaterials: Transmission Line Theory and Microwave Applications*, Wiley-Interscience, Hoboken, 2006.
4. Gennarelli, G. and G. Riccio, "A UAPO-based solution for the scattering by a lossless double-negative metamaterial slab," *Progress In Electromagnetics Research M*, Vol. 8, 207–220, 2009.
5. Zhang, S., W. Fan, K. J. Malloy, S. R. J. Brueck, N. C. Panoiu, and R. M. Osgood, "Demonstration of metal-dielectric negative-index metamaterials with improved performance at optical frequencies," *J. Opt. Soc. Am. B*, Vol. 23, 434–438, 2006.
6. Alù, A., A. Salandrino, and N. Engheta, "Negative effective permeability and left-handed materials at optical frequencies," *Optics Express*, Vol. 14, 1557–1567, 2006.
7. Kussow, A. G., A. Akyurtlu, A. Semichaevsky, and N. Angkawisittpan, "MgB_2-based negative refraction index metamaterial at visible frequencies: Theoretical analysis," *Phys. Rev. B*, Vol. 76, No. 195123, 1–7, 2007.
8. Kouyoumjian, R. G. and P. H. Pathak, "A uniform geometrical theory of diffraction for an edge in a perfectly conducting surface," *Proc. IEEE*, Vol. 62, 1448–1461, 1974.
9. Jun, C. T., Z.-C. Hao, X. X. Yin, W. Hong, and J. A. Kong, "Study of lossy effects on the propagation of propagating and evanescent waves in left-handed materials," *Phys. Lett. A*, Vol. 323, 484–494, 2004.